

## PHOTOLUMINESCENCE, IMPEDANCE, THERMAL CHARACTERISTICS AND HIRSHFELD SURFACE ANALYSIS OF POTASSIUM BISULPHATE SINGLE CRYSTALS FOR THIRD ORDER NLO APPLICATIONS<sup>†</sup>

 **K. Thilaga**<sup>a,d,#</sup>,  **P. Selvarajan**<sup>b,\*</sup>,  **S.M. Abdul Kader**<sup>c,‡</sup>

<sup>a</sup>Research scholar, Reg.No.19221192132006, Department of Physics, Sadakathullah Appa College Tirunelveli -627011, Tamilnadu, India

<sup>b</sup>Department of Physics, Aditanar College of Arts and Science, Tiruchendur -628216, Tamilnadu, India

<sup>c</sup>Department of Physics, Sadakathullah Appa College, Tirunelveli -627011, Tamilnadu, India

(Manonmaniam Sundaranar University, Abishekapatti, Tirunelveli – 627012, Tamilnadu, India)

<sup>d</sup>Department of Physics, Sri S.R.N.M College, Sattur-626203, Tamilnadu, India

\*Corresponding Author: [pselvarajanphy@gmail.com](mailto:pselvarajanphy@gmail.com)

<sup>#</sup>E-mail: [kthilaga@gmail.com](mailto:kthilaga@gmail.com), <sup>‡</sup>E-mail: [aksac.physics@gmail.com](mailto:aksac.physics@gmail.com)

Received October 7, 2021; revised November 12, 2021; accepted December 20, 2021

Good quality potassium bisulphate (KHS) single crystals have been grown by slow evaporation method at room temperature. The KHS crystal was found to be crystallizing in orthorhombic crystal structure with Pbc<sub>a</sub> space group. The photoluminescence behaviour of the crystal was analysed in the visible region. This study disclosed that the grown KHS crystal has intense blue emission peak at 490 nm. Impedance analysis was performed to investigate the frequency dependent electrical characteristics at various temperatures. From the impedance studies the bulk resistance, grain boundary resistance and DC conductivity values of the grown crystal were found out. The KHS crystal was subjected to TGA/DTA and the results have been investigated. The electrical parameters like Fermi energy and average energy gap of KHS crystal have been determined. The evaluated values are used to estimate the electronic polarizability. The intermolecular interactions were predicted using Hirshfeld surface analysis. This analysis exhibited that the utmost contribution to the crystal structure was the K<sup>+</sup>⋯O (46.7%) interaction. The 2D fingerprint plot provides the percentage contribution of each atom-to-atom interaction. Since KHS material is a centrosymmetric crystal, it could be used for third order nonlinear optical (NLO) applications.

**Keywords:** Inorganic crystal; solution growth; XRD; photoluminescence; impedance; TGA/DTA; electronic polarizability; 3-D Hirshfeld surface.

**PACS:** 81.10.Dn, 81.10.-h

In recent years, single crystals with good electrical, thermal, and nonlinear optical properties are in high demand for the development of solid state devices. Accordingly, many researchers have focused on the feasibility and applicability of crystal in the fabrication of devices [1]. Nowadays, the study of NLO materials has garnered much attention since its technological needs are obvious [2]. Some researchers have reported that the inorganic crystals gaining its popularity in the area of nonlinear optics owing to its good physical and chemical stabilities [3]. Many useful inorganic crystals have been discovered and used in laser sources. One such inorganic NLO active substance is potassium bisulphate, often known as potassium hydrogen sulphate (KHS). Though KHS is reusable, affordable, non-toxic and can be employed in both homogeneous and heterogeneous conditions, only few research works have been reported to understand its physical properties. Loopstra has reported the crystal structure of KHS crystal [4]. And the thermoelastic properties of single crystals of KHS have been studied by some investigators [5, 6]. To the best of our knowledge, here we are reporting for the first time the photoluminescence behaviour, electrical properties and intermolecular interactions of the KHS crystal. Also the experimental and theoretical value of density of the KHS crystal has been compared.

### GROWTH OF KHS CRYSTAL

The mixture to grow single crystals of KHS was prepared from high grade potassium hydrogen sulfate using aqueous solution. The solution was stirred for three hours using magnetic stirrer. The prepared mixture was then filtered and placed undisturbed in a reasonably dustless atmosphere. The KHS crystal was harvested within 30 days. The photograph of the grown KHS crystal is shown in Fig. 1.

### RESULTS AND DISCUSSION

#### Structural characterization

The grown KHS crystal was exposed to single crystal X-ray diffraction investigations using MoK<sub>α</sub> radiation ENRAF NONIUS CAD4 diffractometer to identify the crystal system. The data acquired from single crystal XRD investigation displayed in Table 1 shows that the KHS crystal belongs to the orthorhombic crystal system with Pbc<sub>a</sub> space group and 16 molecular units per unit cell. The results of this study appear to be in excellent accord with the published values [4]. Because the Pbc<sub>a</sub> group is a centrosymmetric space group, no second order nonlinear optical (NLO) characteristics will be observed in this sample.

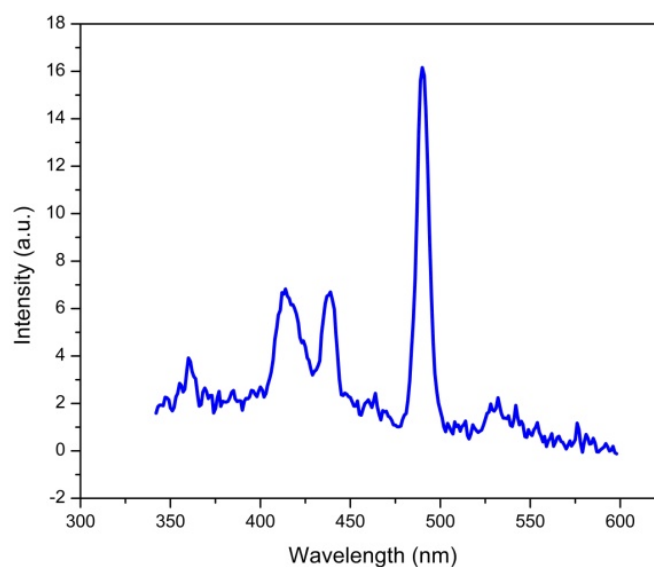
<sup>†</sup> Cite as: K. Thilaga, P. Selvarajan, and S.M. Abdul Kader, East. Eur. J Phys. 4, 145 (2021), <https://doi.org/10.26565/2312-4334-2021-4-19>

© K. Thilaga, P. Selvarajan, S.M. Abdul Kader, 2021

**Figure 1.** Grown crystal of KHS**Table 1.** Single crystal XRD data for KHS crystal

Chemical formula	KHSO <sub>4</sub>
Refinement method	Full matrix Least square method
Molecular weight	136.17 g/mol
Crystal habit	Colorless, transparent
Crystal Symmetry	Orthorhombic
Space group	Pbca
a	8.411(4) Å
b	9.802 (3) Å
c	18.961(2) Å
$\alpha$	90°
$\beta$	90°
$\gamma$	90°
Z	16
Volume of unit cell	1563.23(4) Å <sup>3</sup>
Density	2.313 g/cc

### Photoluminescence studies

**Figure 2.** PL spectrum of the KHS crystal excited at 320 nm.

The PL analysis of KHS single crystal was performed out in the range between 350- 600 nm with an excited wavelength 320 nm and it is shown in Fig. 2. The prepared KHS crystal shows both UV and broad visible emissions. The strength of the peak emitted in the visible range is higher when compared to the UV region. The PL spectrum recorded indicates a less intense UV emission at  $\sim 359$  nm and the blue emission bands at  $\sim 412$  nm,  $\sim 438$  nm and  $\sim 490$  nm. And the emission in the UV and visible region is attributed to the free exciton recombination through an exciton–exciton collision process and the presence of intrinsic defects respectively [7]. The occurrence of charge transfer [8] in the molecules might explain the sharp emission peak at 490 nm. The spectrum indicates that the KHS crystal can be beneficial for fluorescence in blue LED applications [9].

**Impedance Studies**

Impedance analysis was used to understand the electrical behaviour of the KHS crystal. Fig. 3 and 4 depict changes in the real ( $Z'$ ) and imaginary ( $Z''$ ) portions of impedance for the KHS crystal against frequency. As seen in the graph, the real part ( $Z'$ ) of impedance drops as the temperature and frequency rises. Fig. 4 shows that the amplitude of  $Z''$  rises at first, then declines with increasing frequency after reaching a peak ( $Z''_{max}$ ). As the temperature rises, the peak widening and shift to higher frequency regions is observed which shows the presence of an electrical relaxation phenomenon. Moreover, the impedance curves at all temperatures were combined at higher frequency due to a decrease in space charge polarization [10].

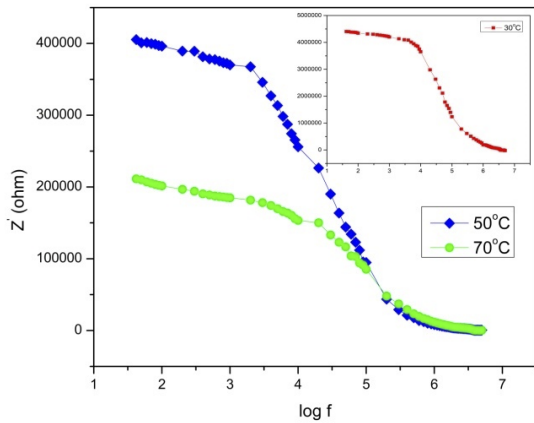


**Figure 3.** Real term of impedance against frequency

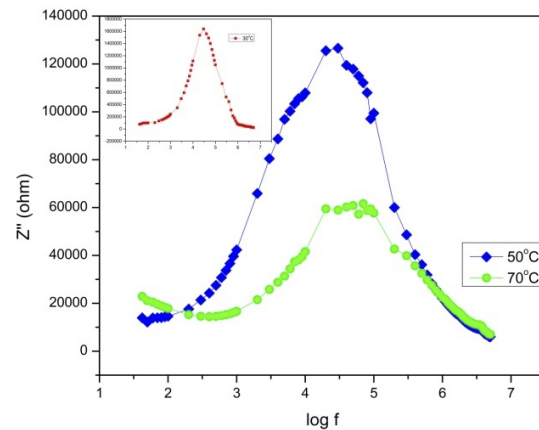


**Figure 4.** Imaginary term of impedance against frequency

Fig. 5 shows the Nyquist plots for the grown KHS crystal between  $Z'$  and  $Z''$  of impedance at various temperatures. The existence of a single semicircular arc and spike suggests that the material's electrical characteristics are mostly attributable to bulk and grain boundary influences [11]. Table 2 shows the bulk resistance  $R_b$  as well as the grain boundary resistance  $R_{gb}$  of the sample derived from the plot. The data clearly shows that when the temperature rises,  $R_b$  and  $R_{gb}$  decreases. Furthermore, this finding supports the insulating nature of KHS sample. Moreover the conductivity of the KHS crystal presented in table 2 was estimated using the formula [12]  $\sigma = d / AR_b$ , where  $A$  is the area of the face of the crystal in contact with the electrode and  $d$  is the thickness of the KHS crystal. The low conductivity of grown KHS crystal supports its quality of dielectric material.

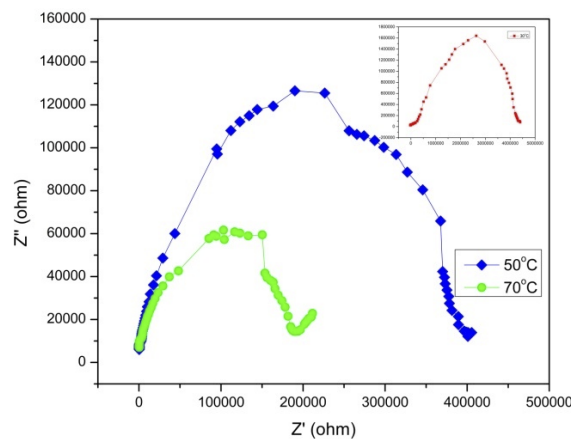


**Figure 5.** Nyquist plot for KHS crystal

**Table 2.** Bulk resistance, grain boundary resistance and DC conductivity values of the KHS crystal

Temperature (°C)	Bulk resistance $R_b$ (ohm)	Grain boundary resistance $R_{gb}$ (ohm)	DC conductivity (ohm m) <sup>-1</sup>
30	$4.40 \times 10^6$	$2.63 \times 10^6$	$2.49 \times 10^{-6}$
50	$4.00 \times 10^5$	$1.90 \times 10^5$	$2.74 \times 10^{-5}$
70	$1.90 \times 10^5$	$1.02 \times 10^5$	$5.76 \times 10^{-5}$

### Thermal studies

The thermal feature of KHS crystal was investigated using the Perkin Elmer STA 600 TG-DTA instrument in the temperature range of 40–730 °C. In a nitrogen environment, the experiment was performed at a pace of 10 °C per minute. Fig. 6 shows the TGA and DTA graph of the KHS crystal. At the beginning of experiment, mass of the sample was 19.90 mg and it had a mass of 14.4 mg at the end. The slight weight loss in the TGA curve over the temperature range 40-50 °C is attributed to the removal of adsorbed water molecules by the sample from the atmosphere. Chemical dehydration is responsible for the endothermic peak at 195°C. And the peak in the DTA curve at 210°C, which corresponds to the weight loss in the TGA curve, indicates simultaneous melting and disintegration of the KHS crystal. The wide peak after the disintegration point is due to the evaporation of gaseous materials [13-15]. Thermal stability of the grown KHS crystal ascertains that they may be used at higher temperatures [16]. The result indicates that 72% of the sample retained even at 720°C. Hence the sample has an imperative quality for device manufacturing.

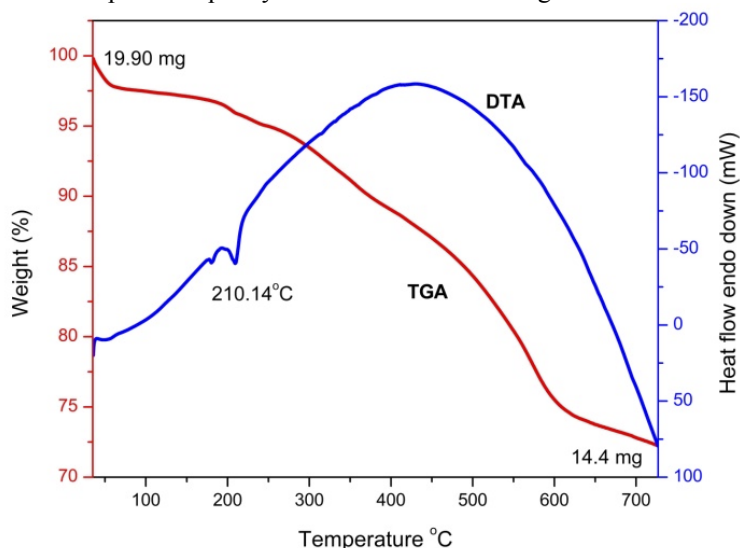


Figure 6. TG/DTA curves for KHS sample

### Electronic polarizability of KHS crystal

The tendency of a charge distribution to be deformed from its usual shape when an electric field is applied to a sample consisting of atoms or molecules is known as electronic polarizability. The estimation of electronic polarizability relies upon certain solid state parameters such as plasma energy of valence electron ( $E_v$ ), Fermi energy ( $E_F$ ) and Penn gap energy ( $E_p$ )

. The value of  $E_v$  is estimated from the following equation

$$E_v = 28.8[(Z' \times \rho)/M]^{1/2}$$

where  $Z'$  is the number of valence electrons of KHS molecule,  $\rho$  is the density of the crystal and  $M$  is the molecular weight of KHS crystal. Here  $M = 136.17 \text{ g mol}^{-1}$ ,  $\rho = 2.313 \text{ g/cc}$ ,  $Z' = 32$ .

Penn gap energy or average energy gap can be estimated using the dielectric constant [17] from the relationship  $E_p = E_v(\epsilon' - 1)^{-1/2}$  where  $\epsilon'$  is the dielectric permittivity, often known as the dielectric constant, has a value of 4.5 at 1 MHz [18]. Fermi energy is the kinetic energy of particles in their most occupied state, and it may be calculated theoretically using the equation  $E_F = 0.2948 \times E_v^{4/3}$ . Table 3 shows the calculated values of  $E_v$ ,  $E_p$ , and  $E_F$  for the KHS crystal.

The electronic polarizability ( $\alpha$ ) of KHS crystal may be determined using the Penn analysis from the relationship

$$\alpha = \left[ \frac{E_v^2 S}{E_v S + 3E_p^2} \right] \times (M/\rho) \times 0.369 \times 10^{-24}$$

where  $S = 1 - (E_p/4E_F) + 1/3(E_p/4E_F)^2$  is a specific constant of the material [19, 20]. The electronic polarizability of the KHS crystal is determined to be  $2.196 \times 10^{-23} \text{ cm}^3$  using Penn analysis.

The value of  $\alpha$  of KHS crystal may also be computed using the Clausius-Mossotti relation given below

$$\alpha = (3M/4\pi N\rho)[(\epsilon' - 1)/(\epsilon' + 2)]$$

where  $N$  is the Avogadro's number [21] and the estimated value of electronic polarizability is  $1.256 \times 10^{-23} \text{ cm}^3$ . The results show that the electronic polarizability of KHS crystal determined using both techniques is almost identical.

**Table 3.** Values of  $E_v$ ,  $E_p$ , and  $E_F$  for KHS crystal

Energy parameters	Values (eV)
Plasma energy ( $E_v$ )	21.233
Penn gap energy ( $E_p$ )	11.350
Fermi energy ( $E_F$ )	17.315

#### Experimental determination of density of crystal

Flotation method was employed to estimate the density of the KHS crystal. A tiny part of crystal was submerged in the mixture of liquid bromoform and carbon tetra chloride in a specific gravity container. When the sample was in the condition of mechanical equilibrium, the density of both the crystal and the combination of liquids would be equivalent. Then using the following relation density can be estimated

$$\rho = (w_3 - w_1)/(w_2 - w_1)$$

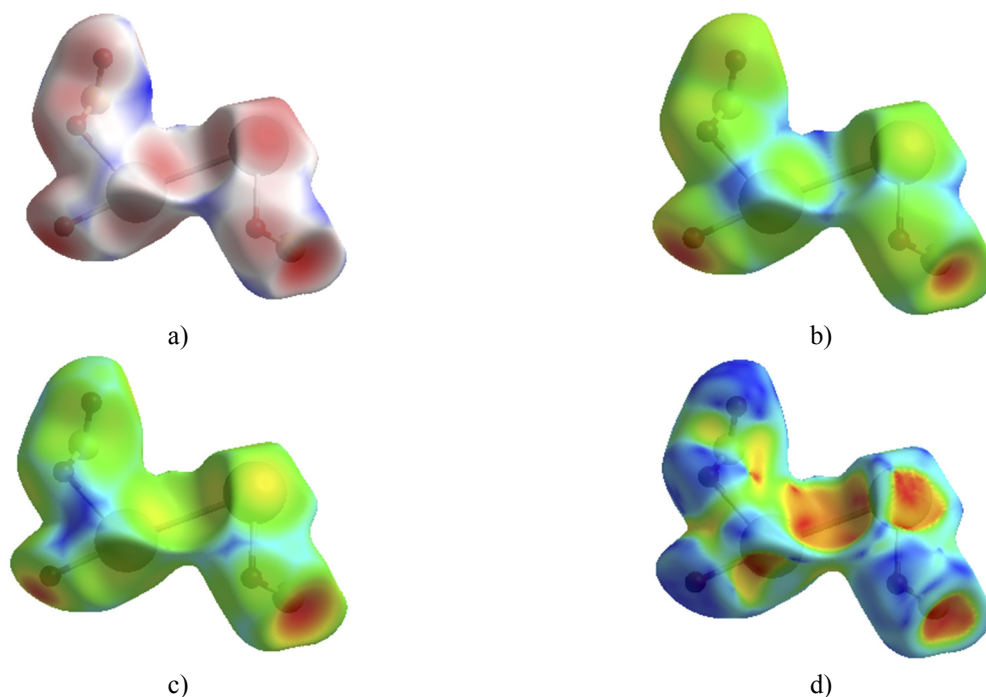
where  $w_1$  represents the weight of a specific gravity bottle,  $w_2$  and  $w_3$  represents the weight of a specific gravity bottle filled with water and the solution mixture respectively. The experimentally estimated density of KHS crystal is 2.325 g/cc, which is nearly identical to the density of KHS crystal, determined using the XRD technique [22].

#### Kurtz-Perry powder technique for SHG

The Kurtz and Perry approach was used to determine the second harmonic generation (SHG) efficiency of the powdered form of the grown KHS crystal [23]. Nd: YAG laser beam ( $\lambda = 1064$  nm) of very high intensity with a pulse length of about 6 ns was incident over the prepared material. The reference sample in this experiment was KDP. The grown crystal was crushed into a powder with a grain size of 300-350 m and the SHG was measured. It is noticed that no green radiation is emitted during the experiment. However, at an input energy of 0.70 J, the typical KDP sample produced green radiation with a SHG signal of 8.90 mJ. From the SHG analysis it is observed that the magnitude of SHG for the KHS sample is zero and is attributed to the centrosymmetric nature of the grown crystal. Third order NLO property (Z-scan) analysis of KHS sample is in progress.

#### Hirshfeld surface analysis

The Crystal Explorer 17.5 programme was used to analyze Hirshfeld surfaces and generate the corresponding 2D fingerprint plots for the KHS crystal. The intercontacts in the KHS crystal were seen utilizing the normalized contact distance  $d_{norm}$ , distance between Hirshfeld surface and the closest atom inside the surface  $d_i$  and distance between Hirshfeld surface and the closest atom outside the surface  $d_e$  maps on the Hirshfeld surface displayed in Fig. 7.

**Figure 7.** The Hirshfeld surface of the compound mapped with a)  $d_{norm}$  b)  $d_i$  c)  $d_e$  d) shape index

The surfaces were made transparent so that molecules and the crystals interacting environment could be seen clearly. The colors red, white and blue in the  $d_{norm}$  mapped Hirshfeld surface show that the interatomic contacts [24-26] are shorter longer, Van der Waals separated and longer respectively. The bright red zone in the  $d_{norm}$  mapping shows the presence of hydrogen bond interactions (S–HO) in the Hirshfeld surface of the investigated crystal. The shape index elucidates molecular packing in more depth. The donor of an intermolecular interaction is represented by the blue bump-shape with a shape-index greater than 1, while the acceptor is represented by the red hollow with a shape-index less than 1. The hydrogen-donor and hydrogen-acceptor groups were represented by the blue and red areas on the shape-index map of KHS crystal displayed in Fig. 7 d). Fig 8 shows a 2D fingerprint plot depiction of a Hirshfeld surface. With 46.7 percent of the Hirshfeld surface of the title molecule, the K...O intercontact makes a significant contribution. Other intercontacts discovered in the Hirshfeld surface of the investigated compound include O...O (27.9%) and S...O (25.4%).

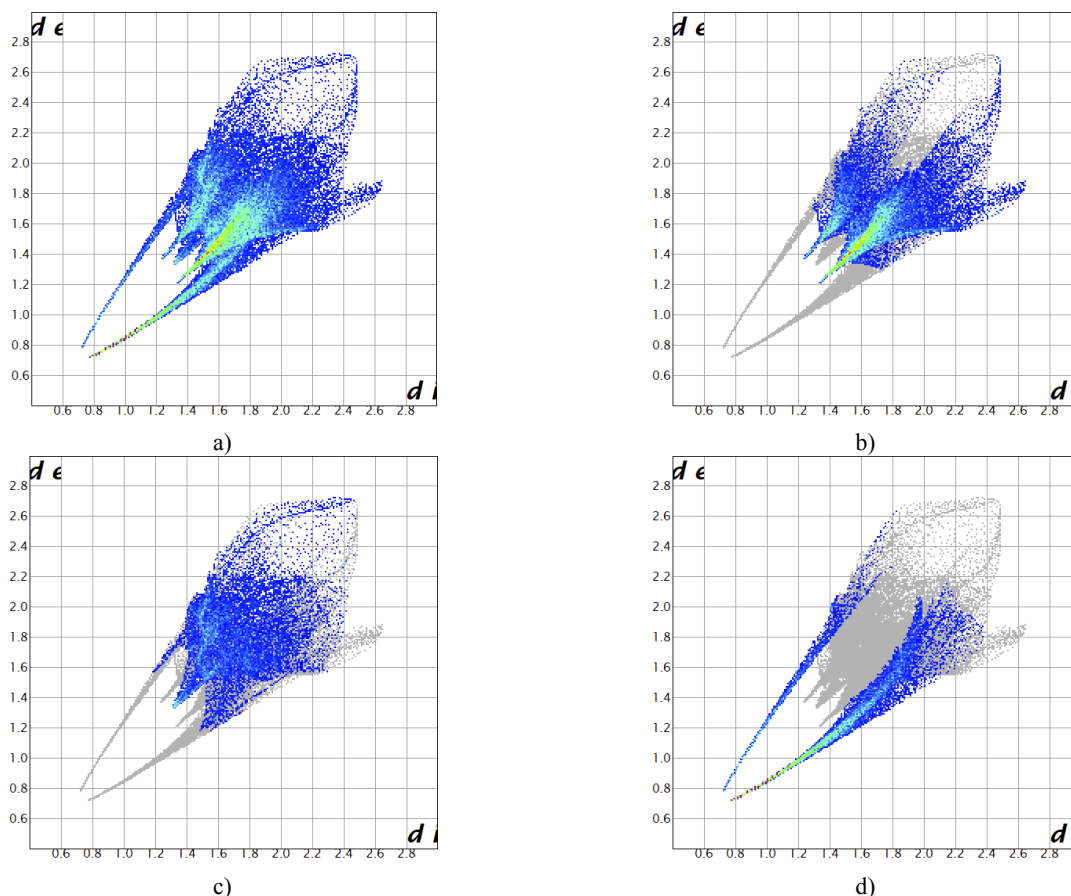


Figure 8. a) title compound b) K...O c) O...O d) S...O interactions and their contribution to the Hirshfeld surface

### CONCLUSION

High optical quality single crystals of KHS were grown by slow evaporation technique. The crystal structure and space group of grown KHS crystal were determined by XRD technique. The photoluminescence feature of the grown crystal indicates that it is appropriate for the photonic devices manufacturing. The electrical properties have been studied using impedance spectroscopic technique and can be used as a tool to identify the good quality dielectric crystal. Thermal steadiness and decomposition point were found by TGA/DTA analysis and it suggests that the sample can be employed for device fabrication. The solid state electronic parameters and the electronic polarizability of KHS crystal were calculated. And the SHG analysis divulges that the KHS crystal is centrosymmetric. The percentages of the intermolecular interactions of the grown sample are revealed using 3D Hirshfeld surface analysis and 2D fingerprint plots.

### Acknowledgement

The authors are thankful to the management of Aditanar College of arts and science, Tiruchendur, Sadakathullah Appa College, Tirunelveli and Sri S. R. N. M College, Sattur for their encouragement to carry out the research work. Also the authors acknowledge the research centers like STIC (Cochin University), St. Joseph's College (Trichy), and Crescent Engineering College (Chennai) for getting the research data of the sample.

### ORCID IDs

K. Thilaga, <https://orcid.org/0000-0003-1124-8733>; P. Selvarajan, <https://orcid.org/0000-0003-1097-4207>  
 S.M. Abdul Kader, <https://orcid.org/0000-0001-6130-3855>

## REFERENCES

- [1] Mohd. Shkir, S. Alfaify, Haider Abbas, and G. Bhagawannarayan, *Materials Chemistry and Physics*, **155**, 36 (2015), <https://doi.org/10.1016/j.matchemphys.2015.01.062>
- [2] P. Maadeswaran, J. Chandrasekaran, S. Thirumalairajan, *Optik - International Journal for Light and Electron Optics*, **122** (3), 259 (2011), <https://doi.org/10.1016/j.ijleo.2009.11.031>
- [3] M.K. Dhatchaiyini, G. Rajasekar, M. NizamMohideen, and A. Bhaskaran, *Journal of Molecular Structure*, **1210**, 128065 (2020), <https://doi.org/10.1016/j.molstruc.2020.128065>
- [4] L.H. Loopstra, and C.H. MacGillavry, *Acta Cryst.* **11**, 349 (1958), <https://doi.org/10.1107/s0365110x58000943>
- [5] D. Gerlich, and H. Seigert, *Acta Cryst.* **A31**, 207(1975), <https://doi.org/10.1107/s0567739475000411>
- [6] J.E. Diosa, R.A. Vargas, E. Mina, E. Torijano, and B.E. Mellander, *Phys. Stat. Sol.* **220**, 641(2000), [https://doi.org/10.1002/1521-3951\(200007\)220:1%3C641::aid-pssb641%3E3.0.co;2-x](https://doi.org/10.1002/1521-3951(200007)220:1%3C641::aid-pssb641%3E3.0.co;2-x)
- [7] P.K. Giri, S. Bhattacharyya, R. Kesavamoorthy, B.K. Panigrahi, and K.G.M. Nair, *Journal of Nanoscience and Nanotechnology*, **9**, 5389 (2009). <https://doi.org/10.1166/jnn.2009.1137>
- [8] S.P. Puppalwar, and S.J. Dhoble, and A. Kumar, *Luminescence*, **26**, 456 (2011), <https://doi.org/10.1002/bio.1252>
- [9] P. Anandan, S. Vetrivel, R. Jayavel, C. Vedhi, G. Ravi, and G. Bhagavannarayana, *Journal of Physics and Chemistry of Solids*, **73**, 1296 (2012), <https://doi.org/10.1016/j.jpcs.2012.06.015>
- [10] J. Uma Maheswari, C. Krishnan, S. Kalyanaraman, and P. Selvarajan, *Physica B: Physics of Condensed Matter*, **502**, 32 (2016), <https://doi.org/10.1016/j.physb.2016.08.042>
- [11] D. Shanthi, P. Selvarajan, and S. Perumal, *Materials Today: Proceedings*, **2**, 943 (2015), <https://doi.org/10.1016/j.matpr.2015.06.013>
- [12] T. Rhimi, G. Leroy, B. Duponchel, K. Khirouni, S. Guermazi, and M. Toumi, *Ionics*, **24**, 1305 (2018), <https://doi.org/10.1007/s11581-017-2306-4>
- [13] P. Karuppasamy, Muthu Senthil Pandian, P. Ramasamy, and Sunil Verma, *Optical Materials*, **79**, 152 (2018), <https://doi.org/10.1016/j.optmat.2018.03.041>
- [14] Z. Sun, G. Zhang, X. Wang, Z. Gao, X. Cheng, S. Zhang, and D. Xu, *Crystal growth & design*, **9**, 3251 (2009), <https://doi.org/10.1021/cg801360q>
- [15] R. Manickam, and G.Srinivasan, *Materials Today: Proceedings*, **8**, 57 (2019), <https://doi.org/10.1016/j.matpr.2019.02.080>
- [16] S. Vedyappan, R. Arumugam, K. Pichan, R. Kasthuri, S.P. Muthu, and R. Perumal, *Applied Physics A*, **123**, 780 (2012), <https://doi.org/10.1007/s00339-017-1394-3>
- [17] P. Karuppasamy, V. Sivasubramani, M. Senthil Pandian, and P. Ramasamy, *RSC Adv.* **6**, 109105 (2016), <https://doi.org/10.1039/c6ra21590d>
- [18] D.R. Penn, *Phys. Rev.* **128**, 2093 (1962), <https://doi.org/10.1103/physrev.128.2093>
- [19] N.M. Ravindra, and V.K. Srivastava, *J. Infrared Phys.* **20**, 67 (1980), [https://doi.org/10.1016/0020-0891\(80\)90009-3](https://doi.org/10.1016/0020-0891(80)90009-3)
- [20] R.R. Reddy, Y. Nazeer Ahammed, and M. Ravi Kumar, *J. Phys. Chem. Solids*, **56**, 825(1995), [https://doi.org/10.1016/0022-3697\(94\)00268-1](https://doi.org/10.1016/0022-3697(94)00268-1)
- [21] R. Robert, C. Justin Raj, S. Krishnan, and S. Jerome Das, *Physica B*, **405**, 20 (2010), <https://doi.org/10.1016/j.physb.2009.08.015>
- [22] C. Krishnan, P. Selvarajan, and T.H. Freeda, *Materials letters*, **62**, 4414 (2008), <https://doi.org/10.1016/j.matlet.2008.07.045>
- [23] S.K. Kurtz, and T.T. Perry, *J. Appl. Phys.* **39**, 3798 (1968), <https://doi.org/10.1063/1.1656857>
- [24] Tarun Kumar Pal, Subrata Paul, Jewel Hossen, Ashrafal Alam, Chanmiya Sheikh, Arkajyoti Paul, and Ryuta Miyatake, *Journal of Molecular Structure*, **1226**, 129397 (2021), <https://doi.org/10.1016/j.molstruc.2020.129397>
- [25] M. Manikandan, P. Rajesh, and P. Ramasamy, *Journal of Molecular Structure*, **1195**, 659 (2019), <https://doi.org/10.1016/j.molstruc.2019.06.001>
- [26] N. Tyagi, H. Yadav, A. Hussain, and B. Kumar, *Journal of Molecular Structure*, **1224**, 129190 (2021), <https://doi.org/10.1016/j.molstruc.2020.129190>
- [27] K. Indira, T. Chitravel, R.R. Saravanan, and P. Indumathi, *Materials Research Innovations*, **23**, 113 (2019), <https://doi.org/10.1080/14328917.2017.1392692>

### ФОТОЛЮМІНЕСЦЕНЦІЯ, ІМПЕДАНС, ТЕРМІЧНІ ХАРАКТЕРИСТИКИ ТА АНАЛІЗ ПОВЕРХНІ ХІРШФЕЛЬДА МОНОКРИСТАЛІВ БІСУЛЬФАТУ КАЛІЮ ДЛЯ ЗАСТОСУВАНЬ NLO ТРЕТОГО ПОРЯДКУ

К. Тілага<sup>a,d</sup>, П. Селварайян<sup>b</sup>, С.М. Абдул Кадер<sup>c</sup>

<sup>a</sup>Дослідник, реєстраційний номер 19221192132006, факультет фізики, коледж Садакатуллаха Анпа Тірунелвелі -627011, Тамілнаду, Індія

<sup>b</sup>Кафедра фізики, Коледж мистецтв і науки Адітанар, Тіручендур -628216, Тамілнаду, Індія

<sup>c</sup>Кафедра фізики, Коледж Садакатуллаха Анпа, Тірунелвелі -627011, Тамілнаду, Індія

(Університет Манонманіам Сундаранар, Абішекапатті, Тірунелвелі – 627012, Тамілнаду, Індія)

<sup>d</sup>Кафедра фізики, Sri S.R.N.M College, Sattur-626203, Тамілнаду, Індія

Високоякісні монокристали бісульфату калію (KHS) були вирощені методом повільного випаровування при кімнатній температурі. Встановлено, що кристал KHS кристалізується в ромбічній кристалічній структурі з просторовою групою P63c. Проаналізовано поведінку фотолюмінесценції кристала у видимій області. Це дослідження показало, що вирощений кристал KHS має інтенсивний синій пік емісії при 490 нм. Для дослідження частотно-залежних електричних характеристик при різних температурах проводили аналіз імпедансу. З досліджень імпедансу були виявлені величини об'ємного опору, опору межзеренних меж і провідності по постійному струму вирощеного кристала. Кристал KHS був підданий TGA/DTA, і результати були досліджені. Визначено такі електричні параметри, як енергія Фермі та середня енергетична ширина кристала KHS. Оцінені значення використовуються для оцінки електронної поляризованості. Міжмолекулярні взаємодії були передбачені за допомогою аналізу поверхні Гіршфельда. Цей аналіз показав, що найбільшим внеском у кристалічну структуру була взаємодія K...O (46,7%). Двовимірна діаграма відбитків надає відсотковий внесок кожної взаємодії атома з атомом. Оскільки матеріал KHS є центросиметричним кристалом, його можна використовувати для нелінійно-оптичних додатків третього порядку (NLO).

**Ключові слова:** неорганічний кристал; зростання розчину; XRD; фотолюмінесценція; імпеданс; TGA/DTA; електронна поляризованість; 3-D поверхня Гіршфельда.